

DESIGN OF AN INTEGRATED ANTENNA FOR AUTOMOTIVE SYSTEMS

R. Azaro, G. Boato, F. De Natale, G. Franceschini, A. Martini, and A. Massa

Department of Information and Communication Technology
University of Trento
Via Sommarive 14
38050 Trento, Italy

Received 11 June 2005

ABSTRACT: This paper describes the design process of an integrated antenna for an automotive rescue system. In order to fulfill the antenna-design requirements in different frequency bands and minimize the interference phenomena arising from the integration of different classes of antennas in a single device, a two-phases stochastic-optimization approach is used. The experimental validation carried out on the developed prototype confirms the effectiveness of the proposed approach. © 2005 Wiley Periodicals, Inc. *Microwave Opt Technol Lett* 47: 513–515, 2005; Published online in Wiley InterScience (www.interscience.wiley.com). DOI 10.1002/mop.21214

Key words: integrated antenna; automotive rescue system; multifunction antennas

INTRODUCTION

An automotive rescue system able to fully exploit available wireless services such as timing, localization, and data exchange (for example, SARSAT, GSM/GPRS, and GPS) requires an antenna system operating in different frequency bands. Due to the automotive-application constraints, important issues arise with regard to the coexistence of more antennas in a limited space as well as limited weight and volume. This paper describes the antenna system developed within the AIDER (accident information and driver emergency rescue) project aimed at developing an accident-management system able to optimize the time and effectiveness of rescue operators. The design of an antenna for each wireless subsystem (COSPAS-SARSAT, GPS, GSM/GPRS) is not critical in itself, while the design of an integrated antenna requires great care so as to avoid mutual-coupling effects arising when the radiating subsystems have to be placed in a single limited volume. Starting from the electrical guidelines of the rescue system and taking into account the geometrical constraints, the antenna design is optimized through a two-phase strategy, as described in the following section. A prototype of the device is built and validated through a set of experimental tests.

ANTENNA DESIGN AND RESULTS

The design of the multifunction antenna was carried out by means of a two-phase process. The first phase is aimed at defining the more appropriate class of antennas for each wireless service by taking into account physical as well as electric constraints. As far as the COSPAS-SARSAT and GSM/GPRS systems are concerned, a monopole antenna turns out to be a good choice. Since the GSM/GPRS system operates in two different frequency bands, a dual-band monopole is adopted by considering a LC tuning device that allows multiband operations. A more demanding task is related to the selection of a proper antenna subsystem for the GPS function. In fact, it is necessary to handle the effects of multipath phenomena caused by reflections and to achieve a hemispherical coverage in order to receive signals from a large number of satellites. A good solution is represented by a right-hand-polarized antenna with a good cross-polarization-rejection ratio

able to discriminate between direct and reflected signals. Since patch antennas are narrowband devices and the resonant frequency varies depending on the ground-plane size as well as on the dielectric loading [1], a conical version of the so-called two-arm Archimedean spiral antenna was chosen. Spiral structures are relatively insensitive to mutual-coupling phenomena [2, 3] and they present a wide hemispherical lobe as well as good cross-polarization-rejection ratios [4].

The second phase deals with the integration of antenna subsystems (defined in the previous phase) in order to find their optimal physical parameters and placement as well as solve interference problems. After the definition of the gain $G(\theta, \varphi, f)$ and the voltage standing wave ratio $VSWR(f)$ of the integrated multifunction antenna, and of the related requirements $G^{\min}(\theta, \varphi, f)$ and $VSWR^{\max}(f)$, with f being the working frequency and θ and φ the angular coordinates, the following cost function is maximized:

$$\Theta(\underline{\kappa}) = \sum_{i=0}^{F-1} \sum_{v=0}^{V-1} \sum_{t=0}^{T-1} \left\{ \max \left[0, \frac{G(t\Delta\theta, v\Delta\varphi, i\Delta f) - G^{\min}(t\Delta\theta, v\Delta\varphi, i\Delta f)}{G^{\min}(t\Delta\theta, v\Delta\varphi, i\Delta f)} \right] \right\} + \sum_{i=0}^{F-1} \left\{ \max \left[0, \frac{VSWR^{\max}(i\Delta f) - VSWR(i\Delta f)}{VSWR^{\max}(i\Delta f)} \right] \right\}, \quad (1)$$

where

$$\underline{\kappa} = \{x_a^{(0)}, y_a^{(0)}, z_a^{(0)} = 0.0, \underline{\gamma}_a; \forall a \in (SRS, GSM/GPRS, GPS)\},$$

and $(x_a^{(0)}, y_a^{(0)}, z_a^{(0)} = 0.0)$ is the location of the a^{th} radiating subsystem on the ground plane. The unknown array $\underline{\gamma}_a$ defines the physical characteristics for each antenna subsystem and in more detail, $\underline{\gamma}_{SRS} = \{l_{SRS}, d_{SRS}\}$ for the SARSAT monopole, $\underline{\gamma}_{GSM} = \{l_{GSM}^{(1)}, l_{GSM}^{(2)}, d_{GSM}, L, C\}$ for the double-band GSM/GPRS monopole, and $\underline{\gamma}_{GPS} = \{r_{GPS}^{(1)}, r_{GPS}^{(2)}, h_{GPS}^{(1)}, h_{GPS}^{(2)}, S_{GPS}, d_{GPS}\}$

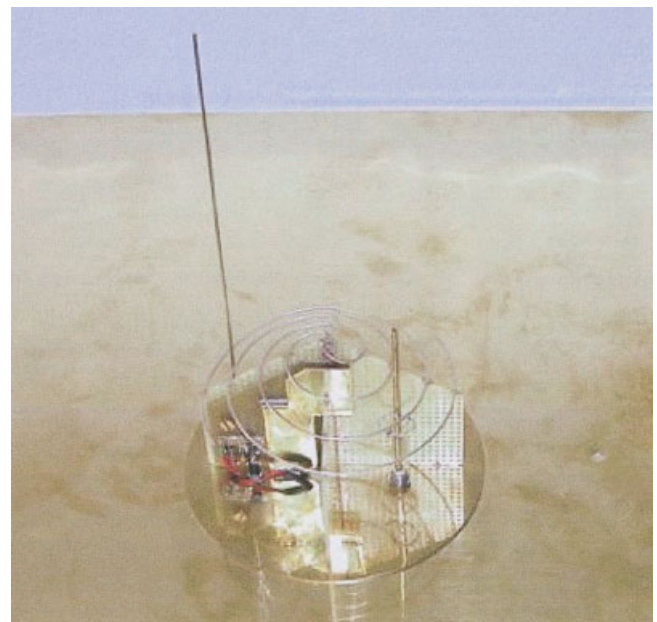


Figure 1 A photograph of a prototype of the multifunction antenna. [Color figure can be viewed in the online issue, which is available at www.interscience.wiley.com.]

antenna gain turns out to be about 6 dB under the required threshold at $\theta = \pm 70^\circ$. Such a result can be considered acceptable, since a preamplification of about 28 dB is required as well. To further assess the reliability of the integrated antenna, the polarization state of the prototype in the GPS band has been evaluated. Results similar to those shown in Figure 4 were also obtained in the orthogonal vertical plane, thus indicating the presence of a circular polarization. For the sake of completeness, Table 1 provides the measured VSWR values as well as the project requirements.

CONCLUSION

The design of an automotive multifunction antenna has been described. The results of the experimental and numerical validations have been reported to confirm the compliance with the specifications as well as the effectiveness of the design procedure.

ACKNOWLEDGMENTS

This work has been partially supported in Italy by the "WILMA—Wireless Internet and Location Management Architecture" Fondo Progetti 2002, Istituto Trentino di Cultura.

REFERENCES

1. N. Padros, J.I. Ortigosa, J. Baker, and M.F. Iskander, Comparative study of high-performance GPS receiving antenna designs, *IEEE Trans Antennas Propagat* 45 (1997), 698–706.
2. J.D. Kraus, *Antennas*, McGraw-Hill, New York, 1988.
3. C.A. Balanis, *Antenna theory: Analysis and design*, Wiley, New York, 1996.
4. D.M. Sazonov, *Microwave circuits and antennas*, Mir Publishing, Moscow, 1998.
5. A. Massa and M. Donelli, A computational approach based on a particle swarm optimizer for microwave imaging of two-dimensional dielectric scatterers, *IEEE Trans Microwave Theory Tech* (to appear).
6. J.R. Robinson and Y. Rahmat-Samii, Particle swarm optimization in electromagnetics, *IEEE Trans Antennas Propagat* 52 (2004), 771–778.

© 2005 Wiley Periodicals, Inc.

PHASE-NOISE REDUCTION OF VOLTAGE-CONTROLLED DIELECTRIC RESONATOR OSCILLATOR FOR THE X-BAND

In-Bok Yom,¹ Dong-Hwan Shin,¹ Keun-Kwan Ryu,² Seung-Hyeub Oh,³ and Moon-Que Lee⁴

¹ Wideband Wireless Technology Research Group, ETRI
161 Kajeong-Dong, Yuseong-gu

Daejeon, 305-350, Korea
² Department of Electronic Engineering
Hanbat National University

San 16-1 Duckmyoung-Dong, Yuseong-Gu
Daejeon, 305-719, Korea

³ Department of Electronics
Chungnam National University

Kung-Dong, Yuseong-Gu
Daejeon, 305-764, Korea

⁴ Department of Electrical and Computer Engineering
University of Seoul

90 Cheonnong-Dong, Dongdaemoon-Gu
Seoul, 130-743, Korea

Received 17 June 2005

ABSTRACT: A different approach for phase-noise reduction of a HEMT VCDRO (voltage-controlled dielectric resonator oscillator) with coupled microstriplines to tune the oscillating frequency is investigated. Two HEMT VCDROs of 9.8 GHz are manufactured in the same configuration, except for the frequency-control circuit, in order to empirically demonstrate the phase-noise reduction. The experimental results show that the phase-noise reduction can be enhanced 8 dBc/Hz at 100-KHz offset frequency by using a frequency-controlled circuit with coupled microstriplines, as compared to the conventional VCDRO. © 2005 Wiley Periodicals, Inc. *Microwave Opt Technol Lett* 47: 515–518, 2005; Published online in Wiley InterScience (www.interscience.wiley.com). DOI 10.1002/mop.21215

Key words: phase noise; DRO; VCDRO; coupled lines

1. INTRODUCTION

The requirements of the local oscillator (LO) in a communication system are high reliability, good stability, low cost, and low phase-noise performance. A dielectric resonator oscillator (DRO) is a cost-effective solution for achieving a highly stable and low phase-noise source in the microwave range [1–3]. Generally, the LO has been achieved as a phase-locked type of oscillator in order to meet the abovementioned conditions [4, 5]. The phase-noise characteristics of LOs depend on that of the reference signal in the loop bandwidth and that of the VCDRO out of bandwidth, respectively.

Generally, the phase noise of a VCDRO is increased along the lower control voltage supply, because the higher capacitance of varactor diodes degrades the loaded quality factor of DRs. To reduce the phase-noise out-of-loop bandwidth, a VCDRO using a different approach with regard to the frequency-control circuit is described in this paper.

2. DIELECTRIC RESONATOR OSCILLATOR DESIGN

In DRO configurations, a popular design topology is the series-feedback type where the transistor is self-biased with the resistor connected to the source of the HEMT. A FHX35LG HEMT fabricated by Fujitsu is used as an active device of the DRO, which is implemented on a 0.385-mm-thick TMM3™ substrate. Figure 1 shows the equivalent circuit of a DR coupled with microstripline and Z_g curves around the resonant frequency. The reactance slope